JOURNAL OF PROPULSION AND POWER
Vol. 10, No. 3, May–June 1994

Vane-Blade Interaction in a Transonic Turbine, Part II: Heat Transfer

K. V. Rao* and R. A. Delaney†
Allison Gas Turbine Division, Indianapolis, Indiana 46206
and
M. G. Dunn‡
Calspan Advanced Technology Center, Buffalo, New York 14225

Part II of this article presents results of a combined computational/experimental investigation into the effects of stator-rotor interaction on the heat transfer distributions on the vane and blade of a transonic turbine stage. The predictions were obtained using a two-dimensional unsteady Navier-Stokes code described in Part I of this article, and the measurements were acquired in a short-duration shock tunnel facility. Twenty miniature thin-film heat flux button gauges were mounted at the midspan of the vane and blade, and contoured inserts containing many thin-film gauges were used on the blade leading edge to spatially resolve the heat transfer rates in that high-gradient region. A grid refinement study was performed with steady noninteractive solutions to ascertain the minimum grid size needed to obtain grid-independent solutions. Predicted time-averaged and phase-resolved heat transfer rates are compared with measurements on the vane and blade.

Introduction

HISTORICALLY, turbine airfoil heat transfer research has received considerable attention because of the strong effect that turbine operating temperature has on engine performance and life. Until recently, the state of the art in airfoil surface heat transfer predictive capability was based on two-dimensional inviscid/boundary-layer methods supplemented by empirical models derived from cascade experiments. In 1983, Hylton et al.[1] assessed the capability of the then available boundary-layer modeling techniques using the STAN5[2] code coupled to an Euler solver. In that study, the Euler/boundary-layer code predictive capability was assessed using cascade data sets by Lander[3] and Turner,[4] as well as a comprehensive data set acquired under the study. Based on the findings of this assessment, modifications were made to models for the transition process, laminar heat transfer augmentation due to freestream turbulence effects, and longitudinal surface curvature effects. From this research, a robust scheme for predicting external convective heat transfer in stationary cascades with attached well-behaved boundary layers was developed.

Limitations in the boundary-layer methods associated with singularities in stagnation and separated flow regions coupled with the widespread use of supercomputers have naturally led to the development of two-dimensional Navier-Stokes codes for the prediction of airfoil surface heat transfer. Boyle[5] and Ameri and Arnone[6] recently reported exceptionally good heat transfer predictive capability for linear cascades with Navier-Stokes codes.

Observed differences between heat transfer levels in stationary and rotating cascades have prompted considerable research in the assessment of unsteady vane-blade interaction effects on turbine heat transfer. Reviews on the unsteady flow in turbine stages and the effect on heat transfer are given by Doorly[7] and Sharma et al.[8] Unsteady heat transfer experiments in large-scale, low-speed rigs have been performed by Dring et al.[9] These experiments have shown considerable unsteadiness on the vane and the blade due to potential and wake interactions. Transonic turbine stage tests performed in short-duration facilities by Dunn et al.[10–12] and Guenette et al.,[13] and rotating bar experiments reported by Doorly and Oldfield,[14] have identified high amplitude unsteady heat transfer rates on the downstream rotating blade row, attributable to interaction with trailing-edge shocks from upstream vanes. Unsteady computational techniques for the prediction of vane-blade interactions have been developed by Rai,[15] Giles,[16] and Lewis et al.[17] These codes have been shown to accurately predict the unsteady aerodynamics and shock structures in transonic turbines. In a first-of-a-kind simulation, Abhari et al.[18] compared heat transfer predictions from the unsteady Navier-Stokes code of Giles[16] with measurements from a transonic turbine test, and showed very little effect of the interaction on the time-mean heat transfer rates on the blade. However, they reported discrepancies between the predictions and data on the blade leading edge due to an underprediction of the vane trailing-edge shock strength.

This article presents results of a computational/experimental investigation of unsteady aerothermodynamics in a transonic turbine stage. Heat transfer data from a full-scale turbine test are compared with results from numerical calculations obtained with the Vane-Blade Interaction (VBI) analysis described in Part I of this article.

A high-pressure turbine was designed and constructed solely for the purposes of this analysis/measurement program. This turbine hardware was instrumented with thin film heat-flux gauges and with flush diaphragm miniature pressure transducers. The measurements were performed using a large shock-tunnel facility that was constructed to accommodate very large weight-flow machines. The turbine stage was installed in the shock-tunnel facility, and detailed time-average and phase-resolved heat flux and surface pressure measurements were obtained for both the vane and the blade. The results of the combined experimental and numerical investigation that were carried out are described in a report by Delaney et al.[19] The surface pressure measurements were presented by Dunn et al.[12] and in Part I of this article.

Received Jan. 19, 1992; revision received Aug. 25, 1993; accepted for publication Aug. 26, 1993.

*Senior Project Engineer, Advanced Turbomachinery Department, P.O. Box 420. Member AIAA.
†Chief, Advanced Turbomachinery Department, P.O. Box 420. Member AIAA.
‡Vice President, Research Fellow, P.O. Box 400. Associate Fellow AIAA.

The computational investigation focused on predicting the steady and unsteady heat transfer rates on the vane and blade of the turbine stage. A systematic grid refinement study was carried out to obtain grid-independent solutions for the steady-state problem. Based on the results from this study, an unsteady calculation was performed using grids which are believed to be adequate for accurately resolving the heat transfer over most of the airfoil surface. Details of the geometry and the flow conditions are given in Part I of this article.

Instrumentation/Measurements

Midspan airfoil surface heat flux distributions on the vane and blade were measured with miniature thin-film gauges. Button gauges were used over the pressure and suction surfaces, and contoured inserts were employed at the leading edges. The particular button gauges used here were made of Pyrex® 7740 and were 0.040 in. in diam and 0.031 in. thick. Platinum strips 0.004 in. wide and 0.020 in. long were painted on the button, and lead wires were attached. After aging the gauge, the unit was calibrated in an oil bath over the temperature range anticipated in the test. The final step was to place the gauges on the airfoils. Figure 1 is a photograph of the button gauges installed on the vane. Twenty gauges were installed along the midspan of the vane, and another twenty were installed along the midspan of the blade. Both the button-type and insert-type heat-flux gauges are installed in the turbine hardware under a microscope. The heat-flux gauges are installed flush with the surface to within less than 2.5×10^{-6} m (0.0001 in.). The surface finish of the Pyrex substrate, on which the thin-film gauge is painted, is on the order of 3×10^{-7} m. The thickness of the platinum film that is painted on the Pyrex is on the order of 1.0×10^{-8} m. The junction between the gauge and the vane (or blade) surface, as well as the surface finish of the Pyrex, are both much less than the roughness corresponding to the surface finish of the metal surface.

Figure 2 is a photograph of the blade showing the leading-edge inserts with the gauges painted on as they were used in these experiments. Contoured leading-edge inserts were employed on the blade leading edge rather than buttons, because of the requirement to not disturb the surface continuity of this highly curved surface. Inserts provide spatially resolved data in this high-gradient heat transfer region. The inserts involved removing a portion of the metal from the leading edge and replacing it with an instrumented Pyrex substrate which contained multiple heat-flux gauges. The Pyrex substrate was contoured to the shape of the leading edge by contouring under a microscope. The part was then notched and platinum thin-film gauges were painted at the desired spacings. The spacing of the gauges corresponds to about 2 or 3% of the wetted distance along the surface. Two blades were instrumented with inserts. On one of the inserts, the gauges were very closely spaced on the suction surface, and

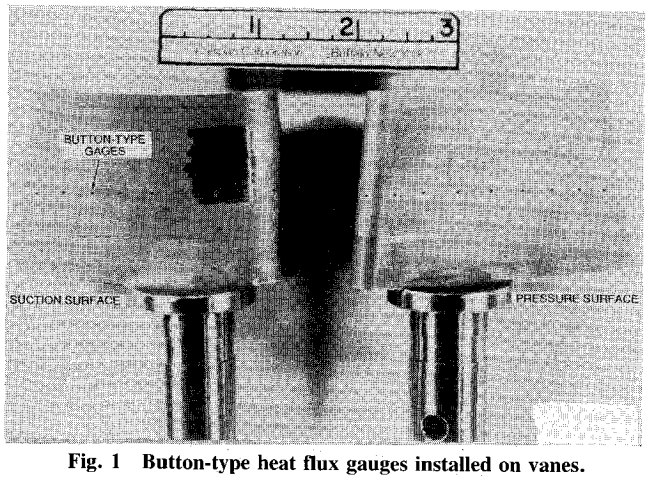

Fig. 1 Button-type heat flux gauges installed on vanes.

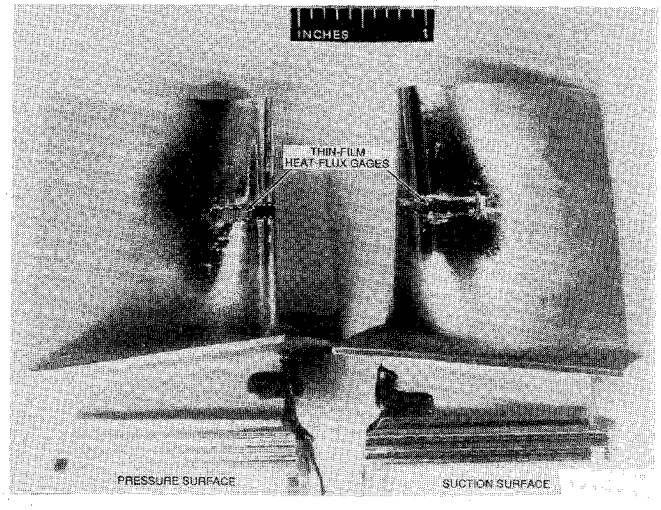

Fig. 2 Leading-edge inserts located at midspan on rotor blades.

were spaced further apart on the pressure surface; the pattern was reversed on the second blade. Because of the 30-vane and 45-blade arrangement, the blades with leading-edge inserts were installed so that they were separated by two blades, and in this way they were always in the same location relative to the vane trailing edge.

The heat transfer results given here are presented in the form of Stanton number based on the conditions at the vane inlet. The Stanton number is evaluated using the relationship

$$St \text{ no.} = \frac{q(T)}{W/A[H_0 - H_w(T)]}$$

where H_0 is the real gas enthalpy at the stage inlet, $q(T)$ is the heat flux evaluated from the one-dimensional heat conduction equation for the thin-film gauge accounting for variable thermal properties at the substrate, $H_w(T)$ is the real gas wall enthalpy evaluated for each gauge at the wall temperature corresponding to $q(T)$, W is the turbine weight flow, T is the thin-film gauge temperature evaluated as a function of time at the sampling frequency, and A is the vane inlet annulus area. The time duration for which the one-dimensional conduction assumption is valid can be estimated using the procedure outlined in Ref. 20. Such an estimate was made for the 0.031-in.-thick Pyrex 7740 buttons used here, and it was determined that the error in heat flux would be less than 1% for a test time of 64 ms. Since the test time for these experiments was significantly less than 64 ms (being on the order of 30 ms), the one-dimensional approximation is considered valid. A previous publication[11] describes sources of uncertainty in the data-acquiring procedure existing at that time. Since Ref. 11 was written, the entire data recording technique has been redesigned and rebuilt to remove many of the potential sources of uncertainty that were cited. The uncertainty in the heat-flux measurements reported in this article is estimated to be ±5%. Further details regarding the measurement/data reduction technique are given by Dunn et al.[11]

Grid Refinement Study

The importance of using adequate grids for resolving heat transfer from airfoils has been emphasized by several researchers. In order to understand the computational grid requirements, a systematic grid refinement study was carried out for the VBI turbine. Steady vane and blade solutions were obtained for the midspan airfoil sections. The study was performed by examining values of the Stanton number along the airfoil surface as the mesh was refined near the wall. A sample O-H grid used in the study is presented in Fig. 3.

Although several grids were used in the study, only results from the final three grids in the refinement study are pre-

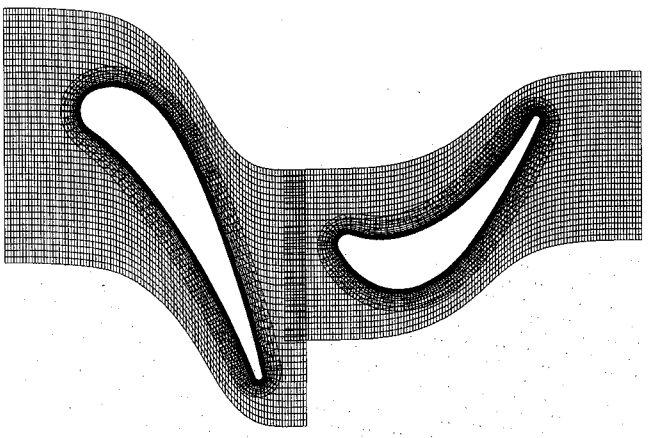

Fig. 3 Grid system for the VBI rig in the closed vane setting.

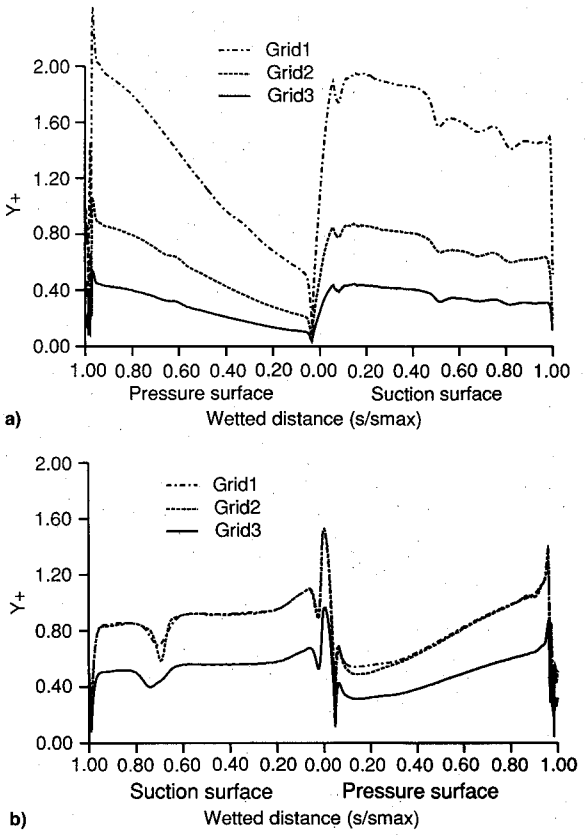

Fig. 4 Variations of y^+ on airfoil surface a) vane and b) blade.

sented here in Figs. 4–7. The grid sizes used in the vane and blade O-grids are given in Table 1. The effect of the refinement is shown in Fig. 4a, which shows the distribution of y^+, which is a measure of the spacing near the airfoil. The grid was refined by approximately halving the spacing near the wall, as shown in Fig. 4a. The effect of this refinement on the pressure distribution along the surface of the airfoils is shown in Fig. 5. The figure shows that the surface pressures were relatively insensitive to the grid size used in this study, and that virtually identical results for the surface pressure distribution along the airfoil surfaces were obtained with all of the grids. The effect of this refinement on the Stanton number distribution along the airfoil surface is plotted in Figs. 6 and 7 for the vane and the blade, respectively. Figure 6 indicates significant differences in the vane Stanton number distribution between grids 1 and 2, and little or no difference between grids 2 and 3. Figure 7 indicates very little difference between grids 1–3, except in the stagnation region near the leading edge of the blade. It can be seen from Figs. 4–7 that as the

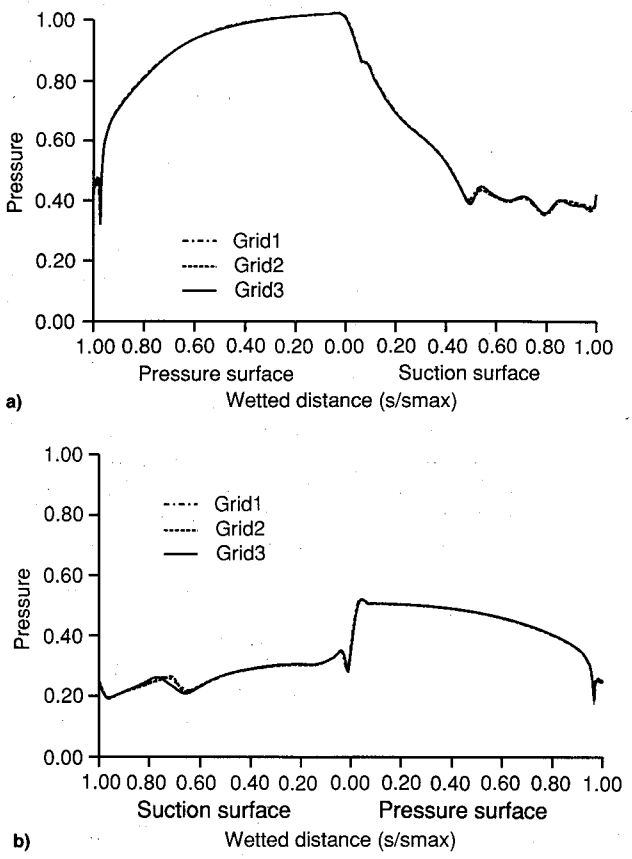

Fig. 5 Surface pressure distribution on airfoil surface a) vane and b) blade.

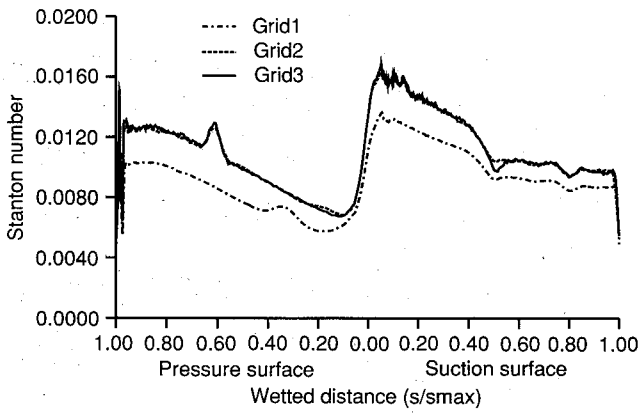

Fig. 6 Stanton number distribution on vane.

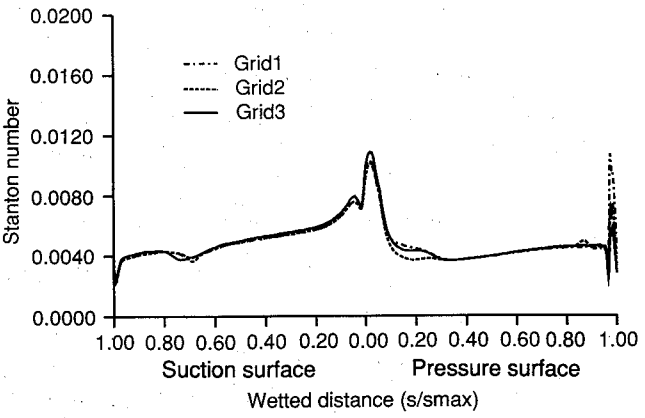

Fig. 7 Stanton number distribution on blade.

Table 1 O-grid dimensions and wall spacing

Vane	Blade
Grid 1 321 × 51, Δy_w = 0.00005	321 × 51, Δy_w = 0.00005
Grid 2 381 × 55, Δy_w = 0.00003	381 × 51, Δy_w = 0.00005
Grid 3 381 × 55, Δy_w = 0.00002	381 × 51, Δy_w = 0.00003

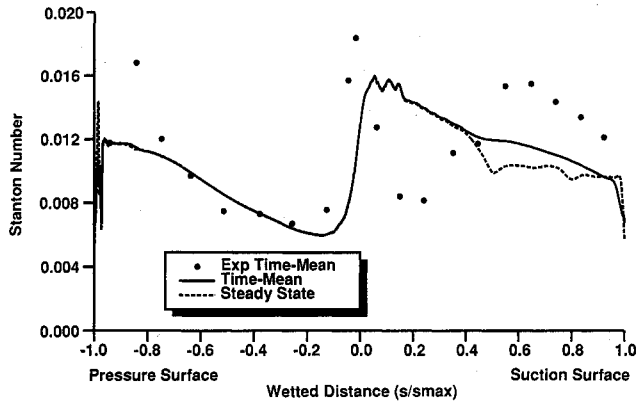

Fig. 8 Time-averaged Stanton number distribution on vane.

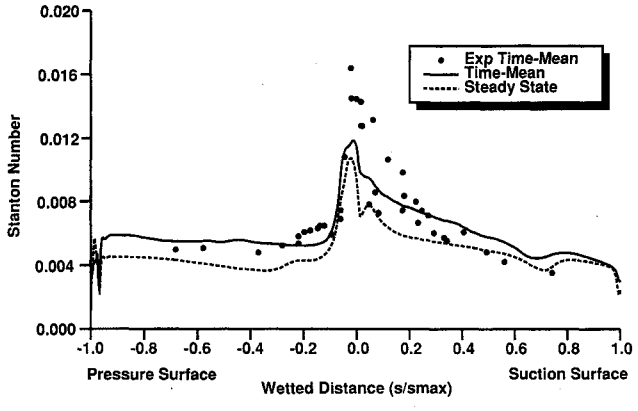

Fig. 9 Time-averaged Stanton number distribution on blade.

value of y^+ is reduced below a certain value ($\approx$1), the dependence of the solution on the grid is eliminated. However, even with the large number of points used in the final grid in this study (labeled grid 3), Fig. 6 shows that in the stagnation region of the blade, grid independence is not achieved. Faced with the increased cost associated with obtaining unsteady solutions on even finer grids, it was decided that the objectives of this study could be accomplished by performing the unsteady calculations with grid 3.

The blip in the pressure side Stanton number of Fig. 6 was created by an inadvertent error in grid generations during these grid refinement calculations. This error was corrected in the final unsteady calculations.

Interactive Results

Figures 8–13 present results from the interactive calculation performed for the VBI transonic stage for the conditions described in Part I of this article. Figures 8 and 9 present the fully turbulent time-averaged and steady-state Stanton number distributions for the vane and the blade, respectively. The Stanton number is presented as a function of percent wetted distance along the airfoil surface. Both experimental data and numerical solutions are plotted on these figures. The steady-state predictions were performed with steady boundary conditions prescribed upstream and downstream of each blade row, assuming no interaction between the rows. Figure 8 shows good agreement between the predictions and the experimental data on the pressure surface of the vane. The dip in the data around 15% wetted distance on the suction surface indicating laminar flow followed by transition to turbulent flow

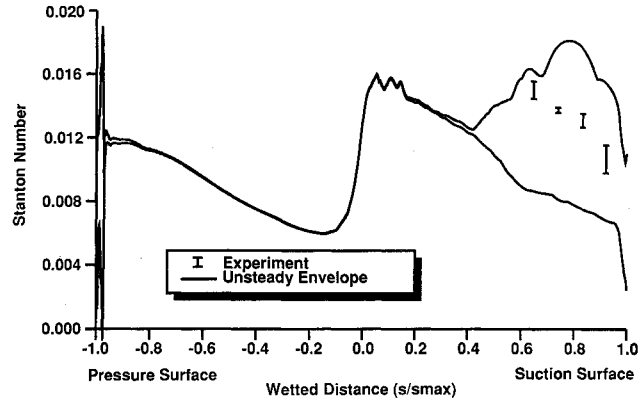

Fig. 10 Unsteady Stanton number distribution on vane.

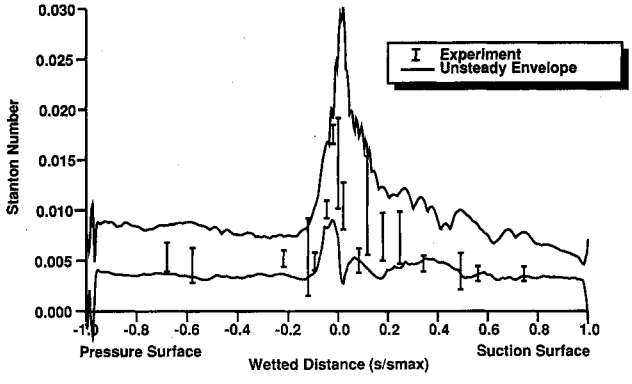

Fig. 11 Unsteady Stanton number distribution on blade.

is not predicted by the fully turbulent analysis. The figure also shows that there is little or no difference between the steady and unsteady predictions on the pressure surface, while there is some difference on the suction surface. This is expected because the vane is choked, and hence, any downstream unsteadiness does not propagate upstream of the throat. The peak Stanton number near the leading edge is underpredicted by the analysis, possibly indicating inadequate grid resolution in that region. From the grid refinement study, this discrepancy is not unexpected, because the grid resolution is lowest in this region. Some of the difference between the experimental data and prediction is attributed to vane-to-vane geometric variations in the size of the vane throat area. The elevated heat transfer levels on the suction surface in Fig. 8 are associated with freestream turbulence. The underprediction of these elevated heat transfer levels indicates the need for better turbulence models to account for the freestream turbulence.

Figure 9 presents the Stanton number distributions along the blade surface. Again, the agreement between the predictions and measurements is reasonable. The trends are similar to those observed for the vane, although the difference between the steady-state and the unsteady predictions is significantly more for the blade with the unsteady prediction giving higher heat transfer levels. This has been observed experimentally by Ashworth et al.[21] and is attributed to the unsteadiness created by the vane wakes and trailing-edge shocks as they are chopped by the rotor blades. The measured points at essentially the same wetted distance near the leading edge on Fig. 9 are the result of measurements on several different blades at nearly the same wetted distance. The result is then an indication of the blade-to-blade heat-flux variation.

Comparisons between the maximum predicted and measured unsteady Stanton number excursions on the vane and the blade are presented in Figs. 10 and 11, respectively. Since the vane is choked for this case, little or no unsteadiness is

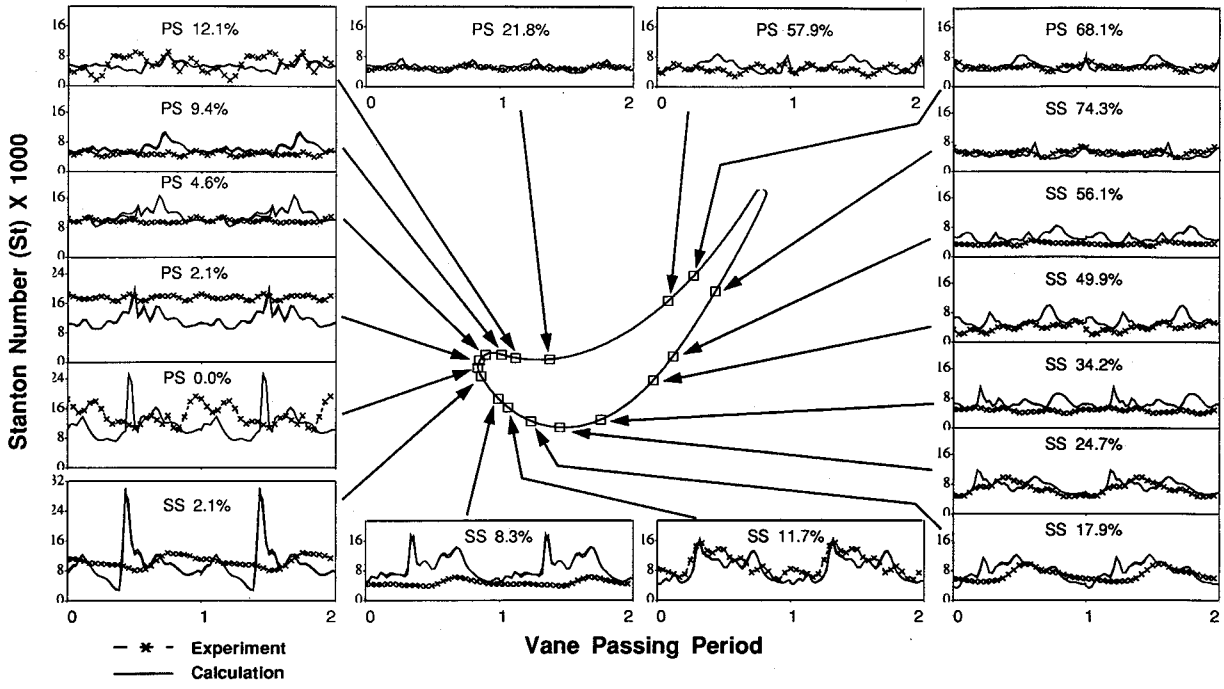

Fig. 12 Phase-resolved Stanton number distributions on blade surface.

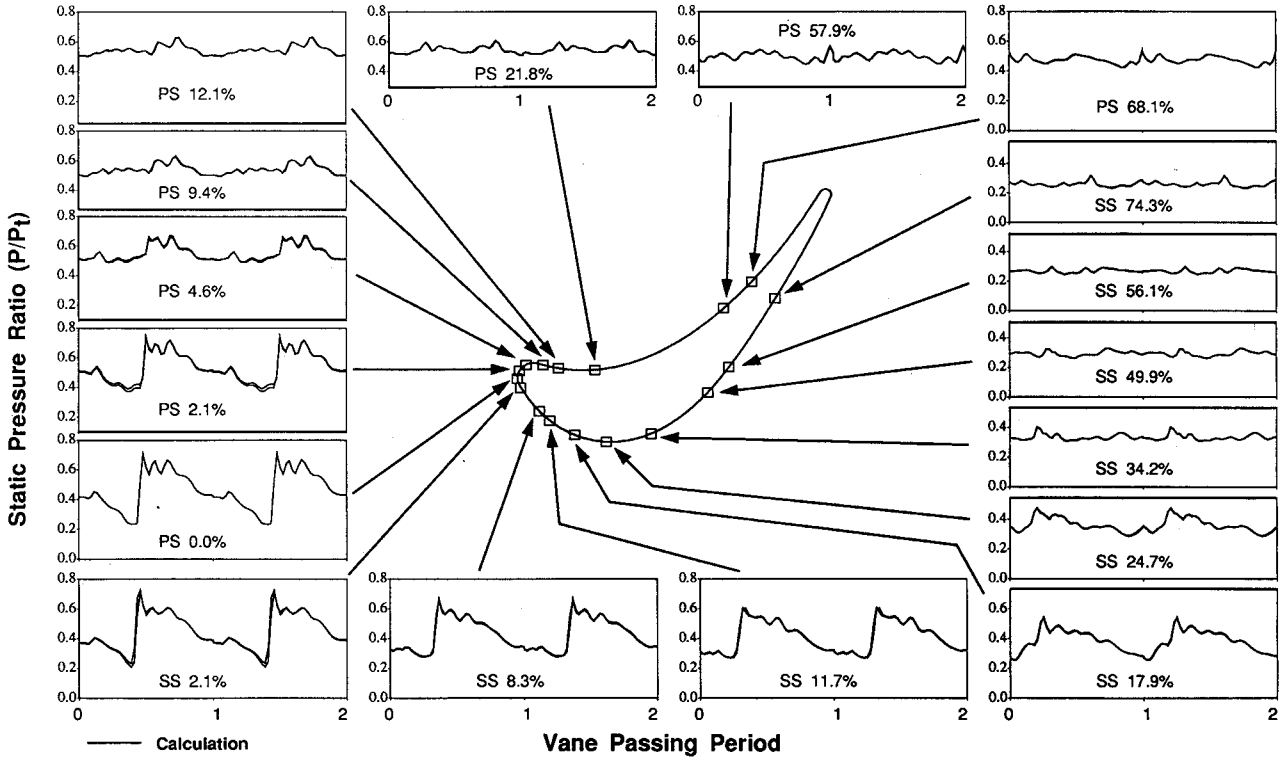

Fig. 13 Phase-resolved pressure distributions on blade surface.

predicted upstream of the vane throat, as shown in Fig. 10. Downstream of the throat on the vane suction surface, the predictions show significantly higher unsteadiness than the data. The reason for this discrepancy is not yet understood. Figure 11 presents the predicted Stanton number envelope for the blade and compares the results with the measurements. The magnitude of the predicted unsteadiness agrees well with the experimental excursions, although the predictions indicate higher unsteady levels than the data. Consistent with the time-mean data in Fig. 8, the predicted leading-edge stagnation point heat transfer level is below the data. Also, the predicted heat transfer levels over the rear portions of the pressure and suction surfaces are above the data.

In order to examine the unsteady phenomena in more detail, blade surface phase-resolved Stanton number data are compared in Fig. 12 with predictions at different blade locations. At each gauge location, the data and predictions from the two grid points nearest to the gauge are plotted. The labels on each plot in this figure indicate the pressure surface (PS) or suction surface (SS), and the percent wetted distance from the geometric stagnation point. The results show no discernible pattern of agreement between data and prediction. In some cases, the predictions agree very well with data, while in other cases, the agreement is poor. In Fig. 12, the beginning and end of a period is chosen arbitrarily so that the calculated phase is best matched with data for most of the gauges. How-

ever, once this reference time is chosen, it is fixed for all locations. From Fig. 12, it appears that some gauges are out of phase relative to the predictions.

In order to investigate the correlation between the heat-flux and the pressure, predicted pressure distributions at the heat transfer gauge locations are plotted in Fig. 13. Figures 12 and 13 show that heat-flux and pressure are in phase over most of the vane passing period. For example, at 11.7% wetted distance on the suction surface, the spike in pressure (Fig. 13) created by the impingement of the vane trailing-edge shock wave produces a corresponding increase in the Stanton number (Fig. 12). Very near the leading edge of the blade, at 2.1% wetted distance on the pressure surface, pressure and heat transfer appear to be out of phase. The reason for this is not understood, although inadequate grid resolution is one possible reason for this difference. In general, the Stanton number is very sensitive to the variations in pressure. Also, Figs. 12 and 13 show variations in Stanton number which do not correspond to any similar variations in pressure. These variations are presumed to be produced by the impingement of the vane wake.

Conclusions

Unsteady heat transfer in a transonic turbine stage was investigated by a time-accurate Navier-Stokes analysis. The predictions were compared with data obtained from a turbine stage which was tested in a short duration shock tunnel. The results show reasonable agreement between data and predictions, with the numerical solutions underpredicting the time-mean, and overpredicting the unsteadiness of the Stanton number distributions on the vane and blade surfaces.

Acknowledgments

This work was funded by Air Force Contract F33615-90-C-2028, Turbine Vane-Blade Interaction. The authors wish to acknowledge the support of R. J. Simoneau of NASA Lewis Research Center for providing computational time on the NAS facility for this investigation. John Griffin provided valuable assistance in preparing figures for this manuscript. The authors would also like to thank Allison Gas Turbine Division and the U.S. Air Force for permission to publish this article. The program monitor was J. H. Friddell.

References

[1]Hylton, L. D., Mihelc, M. S., Turner, E. R., Nealy, D. A., and York, R. E., "Analytical and Experimental Evaluation of Heat Transfer Distribution over Surfaces of Turbine Vanes," NASA CR 168015, May 1983.

[2]Crawford, M. E., and Kays, W. M., "STAN5—A Program for Numerical Computation of Two-Dimensional Internal and External Boundary Layer Flows," NASA CR 2742, Nov. 1976.

[3]Lander, R. D., "Effect of Free-Stream Turbulence on the Heat Transfer to Turbine Airfoils," Air Force Systems Command, Air Force Wright Aeronautical Labs., TR-69-70, Sept. 1969.

[4]Turner, A. B., "Local Heat Transfer Measurements on a Gas Turbine Blade," *Journal of Mechanical Engineering Sciences*, Vol. 13, Jan. 1971, pp. 1–12.

[5]Boyle, R. J., "Navier-Stokes Analysis of Turbine Blade Heat Transfer," American Society of Mechanical Engineers Paper 90-GT-42, June 1990.

[6]Ameri, A. A., and Arnone, A., "Three-Dimensional Navier-Stokes Analysis of Turbine Passage Heat Transfer," AIAA Paper 91-2241, June 1991.

[7]Doorly, D. J., "Modeling the Unsteady Flow in a Turbine Rotor Passage," American Society of Mechanical Engineers Paper 87-GT-197, June 1987.

[8]Sharma, O. P., Pickett, G. F., and Ni, R. H., "Assessment of Unsteady Flows in Turbines," *Journal of Turbomachinery*, Vol. 114, Jan. 1992, pp. 79–90.

[9]Dring, R. P., Blair, M. F., Joslyn, H. D., Power, G. D., and Verdon, J. M., "The Effects of Inlet Turbulence and Rotor Stator Interactions on the Aerodynamics and Heat Transfer of a Large-Scale Rotating Turbine Model, Vol. I—Final Report," NASA CR 4079, UTRC-R86-956480-1, July 1987.

[10]Dunn, M. G., "Detailed Heat-Flux Measurements for the Blade Surface in a Full-Stage Rotating Turbine," American Society of Mechanical Engineers Paper 86-GT-77, June 1986.

[11]Dunn, M. G., George, W. K., Rae, W. J., Woodward, S. H., Moller, J. C., and Seymour, P. J., "Time-Resolved Heat-Flux Measurements for the Rotor of a Full-Stage Turbine: Description of Analysis Technique and Typical Data," American Society of Mechanical Engineers Paper 86-GT-78, June 1986.

[12]Dunn, M. G., Bennett, W. A., Delaney, R. A., and Rao, K. V., "Investigation of Unsteady Flow Through a Transonic Turbine Stage: Part II—Data/Prediction Comparison for Time-Averaged and Phase-Resolved Pressure Data," *Journal of Turbomachinery*, Vol. 114, Jan. 1992, pp. 91–99.

[13]Guenette, G. R., Epstein, A. H., Giles, M. B., Haimes, R., and Norton, R. J. G., "Fully Scaled Transonic Turbine Rotor Heat Transfer Measurements," *Journal of Turbomachinery*, Vol. 111, Jan. 1989, pp. 1–7.

[14]Doorly, D. J., and Oldfield, M. J., "Simulation of the Effects of Shock Wave Passing on a Turbine Rotor Blade," *Journal of Engineering for Gas Turbines and Power*, Vol. 107, Oct. 1985, pp. 998–1006.

[15]Rai, M. M., "Unsteady Three-Dimensional Navier-Stokes Simulations of Turbine Rotor-Stator Interaction," AIAA Paper 87-2058, 1987.

[16]Giles, M. B., "Stator/Rotor Interaction in a Transonic Turbine," AIAA Paper 88-3093, July 1988.

[17]Lewis, J. P., Hall, E. J., and Delaney, R. A., "Numerical Prediction of Turbine Vane-Blade Aerodynamic Interaction," *Journal of Turbomachinery*, Vol. 111, Oct. 1989, pp. 387–393.

[18]Abhari, R. S., Guenette, G. R., Epstein, A. H., and Giles, M. B., "Comparison of Time-Resolved Turbine Rotor Blade Heat Transfer Measurements and Numerical Calculations," American Society of Mechanical Engineers Paper 91-GT-190, June 1991.

[19]Delaney, R. A., Helton, D. J., Bennett, W. A., Dunn, M. G., Rao, K. V., and Kwon, O., "Turbine Vane-Blade Interaction," Vol. I, Wright Research and Development Center TR-89-2154, March 1990.

[20]Vidal, R. J., "Model Instrumentation Techniques for Heat Transfer and Force Measurements in a Hypersonic Shock Tunnel," Cornell Aeronautical Lab. Rept. AD-917-A-1, Feb. 1956.

[21]Ashworth, D. A., LaGraff, J. E., Schultz, D. L., and Grindrod, K. J., "Aerodynamics and Heat Transfer Processes in Transonic Turbine Stage," American Society of Mechanical Engineers Paper 85-GT-128, March 1985.